

Off-Grid Single Phase Micro-Inverter System

Atul S. Lilhare¹, Vaibhav R. Doifode², Prasad B. Joshi³, Pranay S. Shete⁴

Department of Electrical Engineering, Yeshwantarao Chavhan College of Engineering, Nagpur, India¹

Department of Electrical Engineering, Yeshwantarao Chavhan College of Engineering, Nagpur, India²

Department of Electrical Engineering, Yeshwantarao Chavhan College of Engineering, Nagpur, India³

Department of Electrical Engineering, Yeshwantarao Chavhan College of Engineering, Nagpur, India⁴

Abstract— In most of the households appliances, AC electricity are mostly used. This electricity are easily available but renewable energy is increasing now a days as there is shortage of traditional fissile fuel and it also hazardous to the environment. Such form of electricity can be obtained by converting the DC electricity generated by the solar panels using power electronics devices. There are so many types of inverter configuration are available which can be used for such purpose. Dealing with hundreds of watts of energy, micro-Photovoltaic (PV) type inverters can convert solar energy of each PV panel to the utility individually, with significant improvement of overall system reliability and also have a several advantages over the other topology like tuning the output of each panel, less sensitive to overheating problems etc. This paper presents a case study of a single-phase micro-PV inverter. Circuit analysis and its parameters calculation are carried out in details and demonstrated through simulation based on MATLAB/Simulink. The result proves the analysis of the circuit and provides theoretical validation for further work in research.

Keywords— Micro-Inverter; DC-DC converter; H-bridge inverter; MATLAB/Simulink.

I. INTRODUCTION

Power generation from renewable sources is increasing due to several reasons like the shortage of traditional fossil fuel and thermal power generation is hazardous to the environment. Compared to other inexhaustible and clean source such as wind energy, Solar photovoltaic energy is one of the major contributors to renewable power generation. Power electronic inverters are used as an interface while connecting these sources to grid. Since PV modules have relatively low power conversion efficiency, the overall system cost can be reduced using high efficiency power conditioners [1].

In order to convert solar energy to electricity power, inverters ought to be utilized to interface PV modules. According to the past technology, the inverters utilization for PV modules has four types i.e. Centralized inverters; String Inverters; Multi-String inverters and AC module technology. String inverter have a number of PV panels were connected with each other in parallel, through diodes and assembled a PV module in series [2]. This topology provides sufficient voltage to the centralized inverter to avoid voltage amplification and also reach to high power levels to some extent. However, this type of inverter layout contained several limitations [3] like the power loss relatively high due to the mismatch between the PV panels and string diodes; high-voltage dc cables are necessary for connection; moreover, the system design was nonflexible according to the variable environmental conditions (i.e. changeable solar illumination and temperature).

The multi-string inverter in which DC-DC modules are independently operated and one central DC-AC converter is used to interface the common dc-link to the AC grid. In

this type of topology, every string component operates and can be controlled individually. Therefore, it can achieve a higher system efficiency and more flexible design scheme.

AC module technology in PV application is such a system where a PV panel is communicated to a dc-ac inverter directly [4], which is also called AC cell. The inverter presented in this paper falls into this category. This structure integrates the PV module and the inverter into a device. Since there is only a PV module, it has several merits such as no mismatch of losses and easy realization of optimal adjustment between different units.

In general, the DC link voltage of the PV source is lower than the peak grid voltage and their output voltage varies in a wide range according to a two-stage topology that boosts the PV voltage by a dc-dc converter in the first stage and then inverts it into ac voltages in the second stage was reported in [5], [6]. Compared to the mega-watt or kilo-watt central inverters used in PV power plants, modularized PV inverter deals with several hundreds of watts of energy [7]. By doing power conversion individually, the maximum power point tracking (MPPT) efficiency and overall system reliability can be significantly improved.

II. METHODOLOGY

The proposed methodology is explained with the help of following block diagram Fig.1

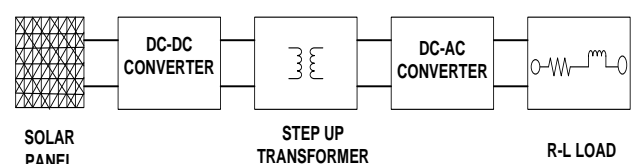


Fig.1 Solar Micro-Inverter Topology

Above block diagram have five terms i.e. solar panel, DC-DC converter, High Frequency Transformer, DC-AC converter and R-L load. Initially Solar panel will generate electricity from sunlight called solar electricity, in this process direct current (DC) electricity is produced. This dc voltage will be converted to pulses using DC-DC converter and then fed to the primary side of the high frequency transformer. This transformer provides galvanic isolation from PV panel to the grid as well as improves the relative high voltage gain. Output of transformer is then fed to the DC-AC converter which converts the DC into AC. Now the output of the micro-inverter supplies the corresponding AC for driving the connected inductive load. In order to run inductive loads a pure sine wave must be generated from inverter to avoid problems related with square wave or modified sine wave inverter. In order to generate a pure sine wave, micro inverter with Pulse Width Modulation (PWM) has been implemented. One stipulation to use PWM is the assumption that the source voltage be larger than the output voltage. This introduces the need for a DC-DC converter which can provide the inverter with a high voltage source. An L-C filter is attached to the inverter output which is parallel to the load, which removes the unwanted harmonics and produces pure sine wave.

III. CIRCUIT ANALYSIS OF A MICRO-PV INVERTER

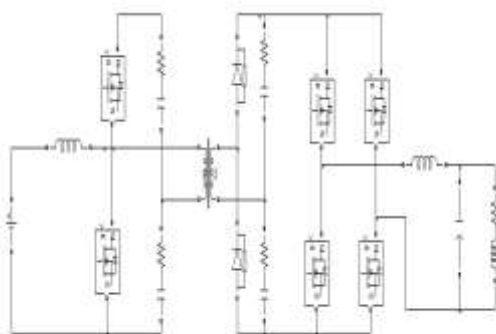


Fig.2 System Configuration of Micro-PV Inverter

Fig. 2 shows the configuration of the presented Micro-PV inverter system. With complementary switching of DC-DC converter, the input voltage V_{in} will be boost to V_{DC} . This dc voltage will be converted to pulses and fed to the primary side of the high frequency transformer. This transformer helps the system to get a relative high voltage gain; besides, it also provides galvanic isolation from PV panel to the grid, which is required by many PV applications. In the studying case, the PV panel output voltage range is from 24 to 80V. A decoupling capacitor is placed in parallel with the PV panel. Input inductor is employed to make the input current ripple under the range

of 30%. Considering its good switching characteristics and low R_d , MOSFET is utilized as switching component. The transformation ratio of the transformer is set as 6. The capacitance of the decoupling capacitor, and the inductance of the input inductor, and the relationship between low-voltage side voltage (i.e. V_{DC}) and input voltage (i.e. V_{in}) will be analyzed in this subsection, respectively.

A. PV Array Modeling

Solar panel has a significant role in designing a microinverter. PV array consists of a number of solar cells in series parallel combination to create rated voltage and current. A solar cell is a PN junction device with non-linear characteristics. Its equivalent circuit can be modelled as shown.

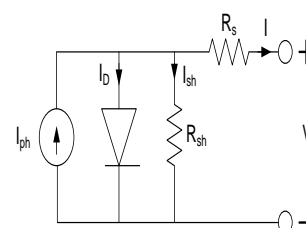


Fig.3 PV Solar Cell

This model consists of a single diode for the phenomena of cell polarization and two resistors (series and shunt) for the losses (Fig. 3). It can thus be named “one diode model”. This model is used by manufacturers by giving the technical characteristics of their solar cells (data sheets). I_{pv} (V_{pv}) characteristic of this model is given by the following equation:

$$I_{pv} = I_{ph} - I_d - I_{Rsh} \dots\dots\dots (I)$$

or, developing the terms I_d and I_{Rsh} :

$$I_{pv} = I_{ph} - I_0 \left[\exp \left(\frac{q(V_{pv} + R_s I_{pv})}{N_s K A} \right) - 1 \right] - \frac{(V_{pv} + R_s I_{pv})}{R_{sh}} \dots\dots (II)$$

The current I_{pv} at the output terminals is equal to the light-generated current I_{ph} , less the diode current I_d and the shunt-leakage current I_{Rsh} . The series resistance R_s represents the internal resistance to the current flow, and depends on the p-n junction depth, impurities, and contact resistance. The shunt resistance R_{sh} is inversely related to the leakage current to ground. In an ideal PV cell, $R_s = 0 \Omega$ (no series loss), and $R_{sh} = \infty \Omega$ (no leakage to ground). In a typical high-quality silicon cell, R_s varies from 0.05 to 0.10 Ω and R_{sh} from 200 to 300 Ω . The PV conversion efficiency is sensitive to small variations in R_s , but is insensitive to variations in R_{sh} . A small increase in R_s can decrease the PV output significantly. In the equivalent circuit, the current delivered to the external load equals the current I_{ph} generated by the illumination, less the diode current I_d and the shunt leakage current I_{sh} . The open-circuit voltage V_{oc} of

the cell is obtained when the load current is zero, i.e., when $I_{pv} = 0$. The shunt resistance (R_{sh}) is very large and the series resistance (R_s) is very small. Therefore, it is common to neglect these resistances in order to simplify the solar cell model. The resultant ideal voltage-current characteristic of a photovoltaic cell is given by the relation below and illustrated by the figure above.

The power-voltage (P-V) characteristic of a photovoltaic module operating at a standard irradiance of 1000 W/m^2 and temperature of 25°C is shown below

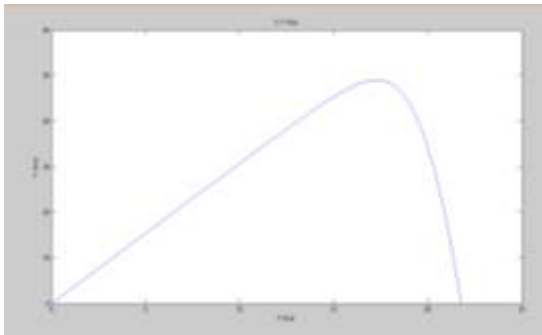


Fig.4 P-V Characteristic of PV Solar Panel

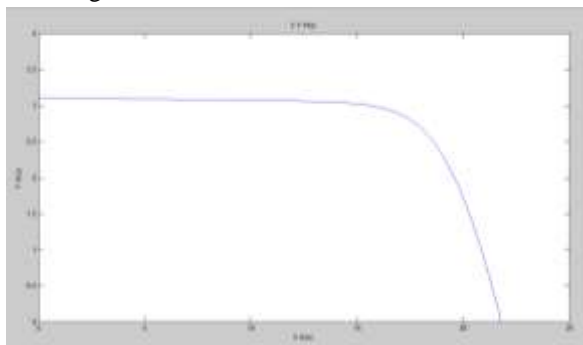


Fig.5 V-I Characteristic of PV Solar Panel

B. DC-DC CONVERTERS

The boost-half-Bridge converter is controlled by S_1 and S_2 with complementary duty cycle. Neglect all switching dead bands for simplifications. When S_1 is ON and S_2 OFF, V_1 is equal to V_{C1} when S_1 is OFF and S_2 is ON, V_1 is equal to $-V_{C2}$. At the steady state, the transformer volt-second is always automatically balanced. In other words, the primary volt-second i.e. positive and negative section are equal, so are the secondary volt-sec i.e. positive and negative section. Normally, D_1 and D_2 are ON and OFF in a similar manner as S_1 and S_2 , but with a phase delay due to the transformer leakage inductance. Ideally, the transformer current waveform is determined by the relationships of V_{C1} to V_{C4} , the leakage inductance, the phase delay, S_1 turn-ON time.

The PV voltage and current are both sensed for calculation of the instantaneous PV power, the PV power variation ΔP , and the PV voltage variation Δv . At the inverter side, the inverter output current I is pre filtered by a first-order low-

pass filter on the sensing circuitry to eliminate the HF noises.

$$V_{C1} = \frac{1-d_1}{d_1} V_{pv} ; \quad V_{C2} = V_{pv} ; \quad V_{DC1} = \frac{V_{pv}}{d_1}$$

$$V_{C3} = \frac{n(1-d_1)}{d_1} V_{pv} ; \quad V_{C4} = V_{pv} ; \quad V_{DC2} = \frac{n.V_{pv}}{d_1}$$

$$V_L(t) = V_m \sin(\omega t) \quad \text{and} \quad I_L(t) = I_m \sin(\omega t)$$

$$P_L(t) = V_L(t) \cdot I_L(t)$$

C. HF TRANSFORMER

The design is based on the specifications reported in Table 1 and has been used to provide the main parameters required by HF transformer manufacturers for the realization of the prototypes.

Table 1

Specification	Value
Turns ratio	6
RMS input current	8.18
Nominal output voltage	230
Minimum output voltage	220
Output current	1.36
Switching frequency	1kHz
Efficiency	98%
Maximum operating flux density	0.05 T
Window utilization	0.3
Duty cycle	0.5
Temperature rise	30°C
Equivalent core section area A_c	170 mm ²
Core volume V_e	14000 mm ³
Mean turn length MLT	71.5 mm
Saturation flux density ΔB	390 mT
Optimum frequency range	0.5-2 kHz
Al	7898.9 nH
Pmax@35 Hz	530 W
Rth	18 °C/W

The design procedure and equations are shown in the section below.

1. Calculation of total transformer power:

$$P_T = \frac{P_{OUT}}{\eta} = \frac{300}{0.98} = 306.12 \text{ Watt}$$

2. Calculation of the number of primary turns:

Assuming a maximum flux density swing of 200 mT, the minimum number of primary turns to avoid core saturation is given by:

$$N_P = \frac{V_{\min_out} \cdot D \cdot T_s}{\Delta B \cdot A_c} = \frac{\left(\frac{220}{2 \times 6}\right) \cdot (0.5) \cdot (28.56)}{(0.25) \cdot 170} = 6.16 \approx 6$$

3. Calculation of the number of secondary turns:

$$N_2 = N_1 \cdot K = 6.6 = 42$$

4. Calculation of the magnetizing inductance:

$$L_1 = N_1^2 \cdot A_l = 36 \cdot (7898.9e^{-9}) \approx 284e^{-6} H$$

5. The primary and secondary winding resistance values are given by:

$$\rho = 0.017 \frac{\Omega}{m} \cdot mm^2$$

$$R_p = \rho \cdot \frac{\lambda_p}{A_{WP}} = (0.017) \cdot \frac{0.85}{0.86} = 16.80m\Omega$$

$$R_s = \rho \cdot \frac{\lambda_s}{A_{WS}} = (0.017) \cdot \frac{6}{0.35} = 291.42m\Omega$$

D. DC-AC INVERTER

In DC-AC converter, S_1 and S_2 are connected in one leg and S_3 and S_4 are connected in the second leg and switch at load frequency, either 50 Hz or 60 Hz. An LCL filter is connected to the mid-point of each inverter leg and is used to interface the system to the load. On the DC side a bank of two electrolytic capacitors is used to store and deliver energy whenever this is required during normal operation. The minimum value of capacitance required on the DC bus is calculated according to the following equation:

$$C_{BUS} = \frac{2 \cdot P_{OUT}}{V_{BUS}^2} \cdot t = \frac{2 \cdot 300 \cdot 10e^{-3}}{220^2} \approx 124 \mu F$$

$$where t = \frac{1}{2f}$$

A total capacitance of about twice the calculated value, rated at 300 V and having an operating temperature of 105 °C, is selected for the inverter implementation. The value of L_f is designed in order to limit the current ripple to about 20% of the nominal current value. The following equations have been used to calculate the filtering inductance value:

$$L_f = \frac{1}{n} \cdot \frac{(V_{BUS} - V_{m-load}) \cdot D}{\Delta i \cdot f_{sw}} = \frac{1}{2} \cdot \frac{(460 - 325) \cdot 0.75}{0.22 \cdot 1e^3} = 230mH$$

where n is the number of inverter levels (+Vbus, 0 and -V) and D is the inverter duty cycle.

The filter capacitor value is selected to limit the exchange of reactive power below 5% of nominal active power:

$$P_{reactive} < 0.05 \cdot P_{active}$$

$$X_{C_f} \geq \frac{V_{load}^2}{0.05 \cdot P_{active}} = \frac{230^2}{15} = 3526.66\Omega$$

$$C_f \leq \frac{1}{\omega \cdot X_{C_f}} = 903.03e^{-9} F$$

To avoid resonance problems for the filter, due to low and high order harmonics, the resonant frequency should be chosen in a range between ten times the line frequency and

one half of the switching frequency. The resonant frequency of an LCL filter is given by:

$$f_{resonance} = \frac{1}{2\pi} \cdot \sqrt{\frac{L_f + L_l}{L_f \cdot L_l \cdot C_f}}$$

IV. SIMULATION AND ANALYSIS

Using MATLAB/Simulink, a detailed model was simulated. The simulation model of the Micro-PV inverter shown in Figure

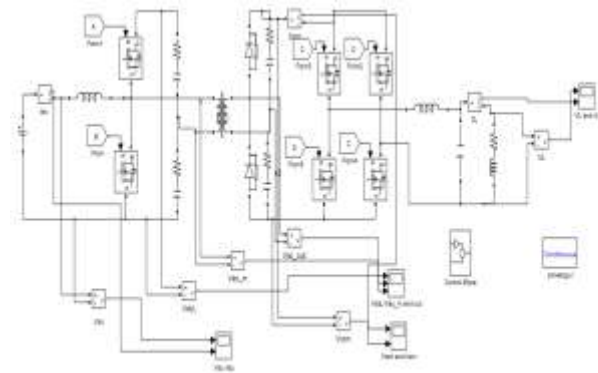


Fig.6 The simulation model of Micro-PV inverter

For simulation purpose, PV cell is replaced by a 24V DC voltage source. The duty cycle of DC-DC converter side is adjusting by the value of PWM technique. The modulation index of SPWM can be adjusted as per requirement of output voltage of DC-AC converter, which stands for the peak value of carrier wave. Thus, the modulation of inverter can output sinusoidal alternating current with different peak values.

Fig.7 shows the result of Output Voltage of PV panel and its current based on the parameters referred above. In order to get the sinusoidal output, the input voltage V_{in} is set to 48V while the duty cycle D of DC-DC converter is set to 50%. The voltage of the low voltage side V_{dc} is about 80-85V and that of the high voltage side is about 210V when the modulation ratio of the inverter is set to 0.9. Due to voltage drop of diodes, transformer and MOSFET, the simulation result V_{out} is slightly lower than the theoretical calculation. Fig.8 shows the result of DC-DC converter voltage along with the voltage of primary and secondary side of transformer. Fig.9 shows the result of voltage and current of half bridge AC-DC converter which is connected across the transformer. This output then fed to full bridge Mosfet based H-bridge inverter where this DC voltage converted to AC voltage which were filtered by LC filter and output is obtain across RL load as shown in Fig.10. Theoretical value and simulated value found to be approximately equal.

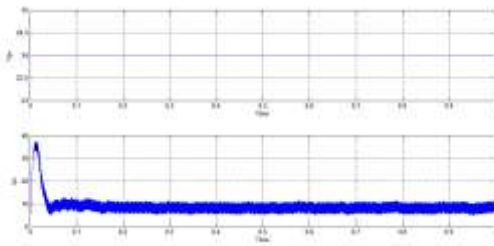


Fig.7 Voltage and Current of PV Solar Panel

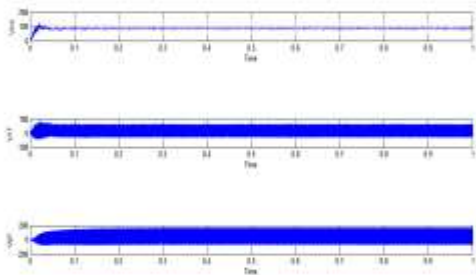


Fig.8 DC-DC Converter and Primary and Secondary HF Transformer Voltage

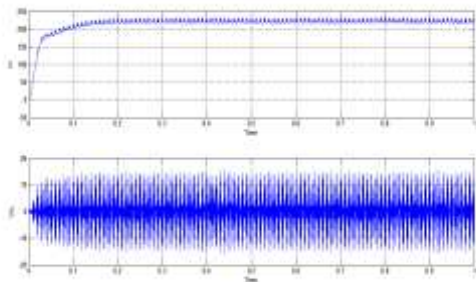


Fig.9 Voltage of Half bridge AC-DC Converter

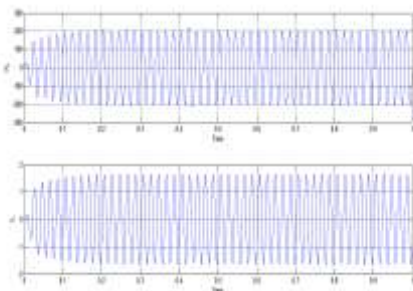


Fig.10 Load Current and Voltage

V. CONCLUSION

This paper presents a Off Grid Single Phase Micro-PV Inverter which use a boost converter integrated with a half-bridge dc-dc converter. Compared to the traditional topology, with a high frequency transformer, the inverter possesses unique merits such as galvanic isolation, reduced numbers of switching devices. Furthermore, the proposed inverter can produce the desirable output voltages by adjusting the duty cycle of the switching devices when the PV cell's output voltage fluctuates. Theoretical analysis of the circuit, parameters calculation and simulation are

presented in this paper. The simulation results provide a validation for the function of the inverter

VI. REFERENCES

- [1] E. Koutroulis, and K. Kalaitzakis, "Development of a micro-controller based photovoltaic maximum power point tracking control system," *IEEE Trans. Power Electron.*, vol. 16, No.1, pp.46-54, January. 2001.
- [2] M. Calais, *et al.*, "Inverters for single-phase grid connected photovoltaic systems-an overview," in *Power Electronics Specialists Conference, 2002. pesc 02. 2002 IEEE 33rd Annual*, 2002, pp. 1995-2000.
- [3] S. B. Kjaer, *et al.*, "A review of single-phase grid-connected inverters for photovoltaic modules," *Industry Applications, IEEE Transactions on*, vol. 41, pp. 1292-1306, 2005.
- [4] M. Wuest, *et al.*, "Single cell converter system (SCCS)," in *Photovoltaic Energy Conversion, 1994., Conference Record of the Twenty Fourth. IEEE Photovoltaic Specialists Conference - 1994,1994 IEEE First World Conference on*, 1994, pp. 813-815 vol.1.
- [5] F. Antunes and A. M. Torres, "A three-phase grid-connected PV system," in *Proc. Ind. Electron. Soc. (IECON 2000)*, vol. 1, pp. 723-728, Oct. 2000.
- [6] J. C. Lima, J. M. Corleta, A. Medeiros, V. M. Canalli, F. Antunes, F.B. Libano, and F. S. Dos Reis, "A PIC controller for grid connected PV system using a FPGA based inverter," in *Proc. Ind. Electron. (ISIE 2000)*, vol. 1, pp. 169-173, Dec. 2000
- [7] Cai Youming , Jia Youwei and Li Yuan, "Circuit Analysis of A Single Phase Micro Photovoltaic Inverter", 978-1-4577-0547-2/12/\$31.00 ©2012 IEEE
- [8] Q. Li and P.Wolfs, "A review of the single phase photovoltaic module integrated converter topologies with three different DC link configurations," *IEEE Trans. Power Electron.*, vol. 23, no. 3, pp. 1320–1333, May 2008.
- [9] R. Wai and W. Wang, "Grid-connected photovoltaic generation system," *IEEE Trans. Circuits Syst.-I*, vol. 55, no. 3, pp. 953–963, Apr. 2008.
- [10] M. Andersen and B. Alvsten, "200W low cost module integrated utility interface formodular photovoltaic energy systems," in *Proc. IEEEIECON,1995*, pp. 572–577.
- [11] A. Lohner, T. Meyer, and A. Nagel, "A new panel-integratable inverter concept for gridconnected photovoltaic systems," in *Proc. IEEE IntSymp. Ind. Electron.*, 1996, pp. 827–831.
- [12] D. C. Martins and R. Demonti, "Grid connected PV system using two energy processing stages," in *Proc. IEEE Photovolt. Spec. Conf.*, 2002, pp. 1649–1652.
- [13] T. Shimizu,K.Wada, andN.Nakamura, "Flybacktype single-phase utility interactive inverter with power pulsation decoupling on the dc input for an ac photovoltaic module system," *IEEE Trans. Power Electron.*, vol. 21, no. 5, pp. 1264–1272, Sep. 2006.
- [14] N. Kasa, T. Iida, and L. Chen, "Flyback inverter controlled by sensorless currentMPPTfor photovoltaic power system," *IEEE Trans. Ind. Electron.*, vol. 52, no. 4, pp. 1145–1152, Aug. 2005.